Relaxation of energy from the transverse to the longitudinal direction of a cold-ion string in a storage ring

Rainer W. Hasse
ESR Division, Gesellschaft für Schwerionenforschung Darmstadt, D-6100 Darmstadt, Germany
(Received 9 April 1992)

With the help of molecular dynamics we study the properties of a string of ions that is confined by an external harmonic potential and that initially is cold in the beam direction but warm in the transverse one. Under the influence of the mutual Coulomb repulsion, intrabeam scattering leads to a flow of energy from the transverse to the longitudinal direction. Depending on the density and the initial transverse temperature $T_{\perp 0}$, three regimes can be distinguished: a fast transient increase of the longitudinal temperature $T_\parallel$ in a fraction of a betatron period, a slow linear increase in some ten betatron periods, and a fast exponential increase followed by complete thermal equilibration. If $T_{\perp 0}$ is large, linear order is lost and thermal equilibrium is postponed to large times. Fourier analyses show that the energy flows into the long-wavelength modes of the collective string excitations. A comparison of calculated heating rates with achievable cooling rates reveals that maintaining linear order in a storage ring is marginal.

PACS number(s): 07.77.+p, 41.75.−i, 41.85.Ja, 29.20.Dh

I. INTRODUCTION

After the recent advent of highly efficient electron coolers in heavy-ion storage rings, Schiffer and Kienle [1], see also Ref. [2], speculated on the possible existence of ordered structures in cold-ion beams. In analogy to the one-component plasma, for a review see Ref. [3], which liquifies at a value of about 3 of the plasma parameter

$$\Gamma = \frac{q^2/d}{kT} \tag{1}$$

(the ratio of Coulomb to thermal energy), where q is the charge ($4\pi\epsilon_0 = 1$), d is the interparticle distance in the laboratory system, and T is the temperature, and which crystallizes at a value of 178 [4], at very low temperature a heavy-ion beam should also be ordered. Since heavy ions can be charged up to $q = 92e$, here the plasma parameter is greatly enhanced due to the quadratic dependence on q in the numerator of Eq. (1). The possible structures of ions confined by a cylindrical harmonic field have been studied extensively [5–8], and range, with increasing density, from the string over a zigzag to helices and intertwined helices. String order and zigzag order of light ions have recently been verified experimentally in a linear Paul trap [9] and string and helical orders in an rf-quadrupole ring trap (ministorage ring) [10], both with laser cooling.

A heavy-ion storage ring, however, is far from being ideal in the sense that the ideal constant radial focusing is only approximately achieved by time-dependent alternate focusing and defocusing. Moreover, it has free drift sections and bending magnets. By the fact that in a constant magnetic field particles run on displaced circles with the same radius, particles that once were beside each other, after 90° of deflection tend to be located one behind the other. This creates strong shearing forces in the crystal that break it and that increase the temperature irreversibly. Idealized computer simulations with alternate bending and focusing-defocusing [11, 12] are not yet decisive. Essentially no stable three-dimensional structure has yet been identified experimentally or in a computer simulation with a realistic lattice of a storage ring [13]. However, it cannot be excluded that *local* order has already been produced in the Heidelberg test storage ring TSR, where light ions were cooled by laser cooling to very low longitudinal temperature [14, 15].

If all particles run on the central orbit bending forces cannot build up. One therefore expects that a linear string of particles can survive in a storage ring, provided that the longitudinal and transverse temperatures can be maintained at a low enough level in the liquid or crystalline regimes.

Longitudinal electron cooling is more effective than the transverse one by the factor [16]

$$\frac{kT_\parallel^{\rm el}}{kT_\perp^{\rm el}} = \frac{kT_\perp^{\rm el}}{8E_0^{\rm el}}\frac{\gamma+1}{\gamma^2},$$

where $E_0^{\rm el}$ is the electron-beam energy and γ is the relativistic Lorentz factor. This manifests itself also in a lower ion temperature in the beam direction as compared to the transverse one,

$$kT_\parallel = E_0(\Delta p/p)^2, \qquad kT_\perp = 2E_0\epsilon Q\gamma^2/\ell,$$

where E_0 is the ion-beam energy per particle, $\Delta p/p$ is the momentum spread, ϵ and Q are the emittance and betatron tune, and ℓ is the circumference of the storage ring. At the experimental heavy-ion storage ring (ESR) at GSI Darmstadt with $\ell \approx 100$ m and $Q \approx 2$ after electron cooling (with a cooling time of about 5×10^4 betatron periods), one expects, for a uranium beam at 100 MeV, an emittance of better than 0.05π mm mrad and a momentum spread smaller than 5×10^{-6} [17]. One could form a string of 2×10^6 particles with an interparticle distance

of $d=50$ μm, and hence an interion Coulomb energy of $q^2/d \approx 0.25$ eV and ion temperatures of $kT_\parallel \approx 5$ meV and $kT_\perp \approx 2.5$ eV at $\gamma = 1.5$. This yields plasma parameters of the order of $\Gamma_\parallel \approx 50$ and $\Gamma_\perp \approx 0.1$. The estimates above, however, are based on higher particle densities in the three-dimensional (3D) gaseous regime and the Γ values at 1D string densities can be higher.

The purpose of this paper therefore is to investigate the question of the flow of energy from the warm transverse (horizontal and vertical) degrees of freedom into the cold beam direction. With the help of molecular-dynamics (MD) calculations we study the increase of temperature in the beam direction by Coulomb scattering of particles in a box with periodic boundary conditions and extract the time rates of change as functions of the initial transverse temperature and density. Simple formulas for the heat energies and the heating rates are extracted either from analytical models or from fits to the MD data. In Sec. II the MD dynamics method is outlined and in Sec. III general results are stated. Subsequently, Secs. IV–VII deal with transient heating, heating rates, thermal equilibrium, and collective vibrations, respectively. In Sec. VIII the calculations and results are summarized and implications on the possible experimental verification are discussed. Mathematical details can be found in Appendixes A–C.

Similar studies have been performed by Schiffer and Hangst [18]; however, with the main emphasis on the influence of different focusing constants in the two transverse degrees of freedom; and by Armbrüster *et al.* [19] for homogeneous systems at higher temperatures. In this context the collective excitations of a warm string in a storage ring were investigated by Avilov and Hofmann [20].

II. MOLECULAR DYNAMICS

In the MD calculations we simulate the infinitely long string of ions by N particles with the average distance d along the beam direction in a box with periodic boundary conditions. Denoting by $\mathbf{x}$, $\mathbf{y}$, $\mathbf{z}$, $\boldsymbol{\rho}=\mathbf{x}+\mathbf{y}$ and $\mathbf{r}$ the horizontal, vertical, longitudinal (beam), transverse directions, and the coordinate, respectively, the focusing and Coulomb forces act on the particle i,

$$\mathbf{F}^i_{\text{foc}} = -m\omega^2_{\beta x}\mathbf{x}_i - m\omega^2_{\beta y}\mathbf{y}_i,$$
$$\mathbf{F}^i_{\text{Coul}} = -q^2\boldsymbol{\nabla}_i \sum_{j>i} |\mathbf{r}_i - \mathbf{r}_j|^{-1}. \tag{2}$$

The latter is replaced by standard Ewald summation, details of which can be found in Ref. [7]. Since mostly $\omega_{\beta x} \approx \omega_{\beta y}$ we define by $2\omega^2_\beta = \omega^2_{\beta x} + \omega^2_{\beta y}$ the average betatron frequency, and $T_\beta = 2\pi/\omega_\beta$, the average betatron period, is the time scale for transverse motion. With the help of the frequency unit

$$\omega_0 = \sqrt{q^2/m\gamma^3 d^3},$$

where γ is the Lorentz factor, see Appendix A, $T_0 = 2\pi/\omega_0$ is the Coulomb period, the time scale for longitudinal motion, and we define the dimensionless linear density

$$\lambda = \frac{\sigma a_{\text{WS}}}{q} = \frac{a_{\text{WS}}}{d}$$

as the particle density σ/q times the Wigner-Seitz radius,

$$a_{\text{WS}} = \left(\tfrac{3}{2}q^2/m\omega_\beta{}^2\right)^{1/3}. \tag{3}$$

Here $\lambda_{\text{crit}} = 0.709$ is the maximum linear string density where the string loses its stability with respect to the zigzag configuration, see Appendix A. In the following we will be mainly concerned with intermediate densities of $\lambda = 0.45$. Note, however, that the linear particle density remains constant for given distance d, so that in the string region λ instead is a measure for the focusing strength or for the betatron frequency,

$$\tfrac{2}{3}\lambda^3 = \omega_0^2\ \omega_\beta^{-2}. \tag{4}$$

The initial conditions are specified as random initial velocities and displacements in the transverse degrees of freedom within a Boltzmann distribution, thereby disregarding the Coulomb potential, but only as random or vanishing initial displacements from the ultracold string in the beam direction. Hereby, the longitudinal and transverse dimensionless temperatures $\Theta_\parallel$, $\Theta_\perp$ are defined as the respective kinetic energies per degree of freedom in units of $\epsilon_0 = q^2/\gamma^3 d \equiv m\omega_0{}^2 d^2$, viz.,

$$\tfrac{1}{2}\Theta_\parallel \epsilon_0 = \tfrac{1}{2}m\langle \dot{z}^2\rangle, \qquad \Theta_\perp \epsilon_0 = \tfrac{1}{2}m\langle \dot{\boldsymbol{\rho}}^2\rangle, \tag{5}$$

so that thermal equilibrium implies $\Theta^{\text{TE}}_\parallel = \Theta^{\text{TE}}_\perp \equiv \Theta$,

$$\tfrac{3}{2}\Theta\epsilon_0 = \tfrac{1}{2}m\langle \dot{\mathbf{r}}^2\rangle.$$

Furthermore, denoting by $\Theta_{\parallel 0}$ and $\Theta_{\perp 0}$ the respective temperatures at time zero with $\Theta_{\perp 0} \gg \Theta_{\parallel 0}$ and disregarding changes of the potential energy, the final temperature will be $\Theta = \frac{2}{3}\Theta_{\perp 0}$. We shall use the terms *temperature* and *kinetic energy* (per particle) synonymously. In this notation, the plasma parameter (1) is the reciprocal of the dimensionless temperature. Note however, that the definition of Γ in the literature is not unique. If dealing with a 3D one-component plasma it is more convenient to employ the Wigner-Seitz radius (3) in the definition (1). Also, the Lorentz factor can be incorporated by replacing d by $\gamma^3 d$. This gives an uncertainty in the numerical value of Γ of the order of a factor of 5. Here we consider initial transverse plasma parameters of the order of 0.1–30 in the gaseous and liquid regimes. In this notation, the average square transverse amplitude ($\rho = |\boldsymbol{\rho}|$) and the average square distance between two particles are

$$\langle \rho^2\rangle = \tfrac{4}{3}\lambda^3\Theta_\perp d^2,$$
$$\langle s^2\rangle = \left(1 + \tfrac{8}{3}\lambda^3\Theta_\perp\right) d^2. \tag{6}$$

III. GENERAL RESULTS

In most of the calculations $N = 64$ particles in the box sufficed because comparisons with results with larger particle numbers ($N=512$) essentially did not change. If not otherwise noted, in the following we will use $N = 64$. However, for small numbers of ions the statistical fluctuation of the energy is larger, $\propto N^{-1/2}$. For $N = 64$, for instance, the width of the energy distribution for given initial temperature is about $\pm 20\%$, in contrast to $\pm 8\%$ for $N=512$. This manifests itself also in a relatively large spread of the final temperature.

A typical example of a MD calculation with 64 ions is shown in Fig. 1. Starting with $\Theta_{\|0} = 0$ and $\Theta_{\perp 0} = 4.2$ and various seeds for the random number generator the transverse kinetic energies oscillate about their mean values and the longitudinal one increases in time. The final spread of $\Theta_{\|}$ is of the order of $\pm 20\%$, in accordance with the same initial spread. Since in the following only one particular initial condition will be used, all results hence are only accurate within this error.

In the schematic calculations of Ref. [18] emphasis was put on the fact that the motion of particles in a two-dimensional potential with a rational ratio of frequencies is periodic but otherwise chaotic. Results showed that more energy is transferred faster from the transverse to the longitudinal direction if the ratio of betatron frequencies is 19 : 21 rather than 9 : 10, with the least energy being transferred for a ratio of 1 : 1. This was explained with the reasoning that the chance for a close collision is smaller if the motion is periodic. Figure 2 shows our results for an intermediate density of $\lambda = 0.45$ and intermediate initial transverse temperature of $\Theta_{\perp 0} = 2.1$ and $\Theta_{\|0} = 0$, but with various ratios $\omega_{\beta x} : \omega_{\beta y}$. As a result, also the least energy is dissipated for a ratio of 1 : 1 but the increase in heat energy is monotonic with increasing ratio $\omega_{\beta x} : \omega_{\beta y}$ (or $\omega_{\beta y} : \omega_{\beta x}$), regardless of the rationality or nonrationality of the ratio (19 : 20 is close to $3:\pi$). An analysis of these results revealed that the phase relations between the horizontal and vertical motion are lost after a few betatron oscillations. The remaining effect of increased heating for ratios not close to unity then is attributed to the increased scattering rate

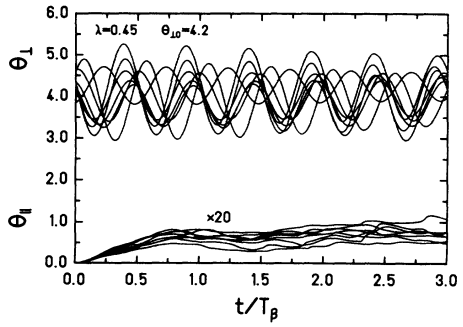

FIG. 1. Transverse ($\Theta_\perp$) and longitudinal ($\Theta_\|$) temperatures vs time (in units of the betatron period) for various random initial conditions with the same initial $\Theta_{\perp 0}$ and $\Theta_{\|0}=0$ ($N=64$ particles in the box).

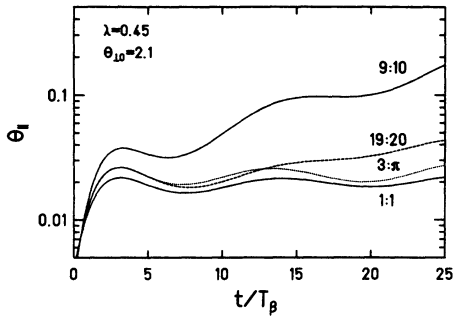

FIG. 2. Increase of longitudinal temperature vs time for various ratios $\omega_{\beta x}:\omega_{\beta y}$ and the same initial temperatures in the two transverse degrees of freedom. For clarity, the curves have been smoothed by polynomial fits.

between particles in the compressed degree of freedom with the larger betatron frequency and smaller average amplitude. In order to simulate the influence of different focusing and defocusing in the following we shall use the ratio $\omega_{\beta x}^2:\omega_{\beta y}^2 = 19:21$ throughout.

Figure 3 shows the change of transverse to longitudinal kinetic energy for a density of $\lambda = 0.45$ followed in time for 50 betatron oscillations. The initial longitudinal energy is always zero and the initial transverse energy varies from 1.2 to 27.4. According to Eq. (6) for this density the average transverse amplitude becomes larger than the cold interparticle distance d at $\Theta_{\perp 0} > 8.2$. The beat in $\Theta_\perp$ stems from the different betatron frequencies in the two transverse directions as stated above. In general, the longitudinal heat is increasing monotonically apart from the statistical fluctuations. However, there are also strong fluctuations, e.g., in the case $\Theta_{\perp 0} = 4.2$, which come from single close encounters of two particles.

One observes different regimes of heating on different time scales: (i) For all initial transverse temperatures there is a fast transient heating of the longitudinal degree of freedom to a plateau value in a time of up to one betatron period; (ii) for relatively small $\Theta_{\perp 0}$ there follows a region of several to some ten T_β with an approximately linear heating rate; (iii) this is followed by a very fast (approximately exponential) heating up to thermal equilibrium about on the same time scale; (iv) if the initial $\Theta_{\perp 0}$ is relatively large the linear and exponential heating regimes are missing and the thermal equilibrium is postponed to very large times or might even not be attained asymptotically. These different regimes will be discussed separately in the next sections.

IV. TRANSIENTS

Since the 1D longitudinal system and the 2D transverse system were prepared at time zero separately the joint system first relaxes very fast to a common 3D system. Depending on the density this transient heating to a plateau value happens on a very short time scale of the order of a fraction of the betatron period [21]. Independent of the density the theoretical value, see Appendix B,

$$t^{\text{trans}} = 0.08 T_0, \tag{7}$$

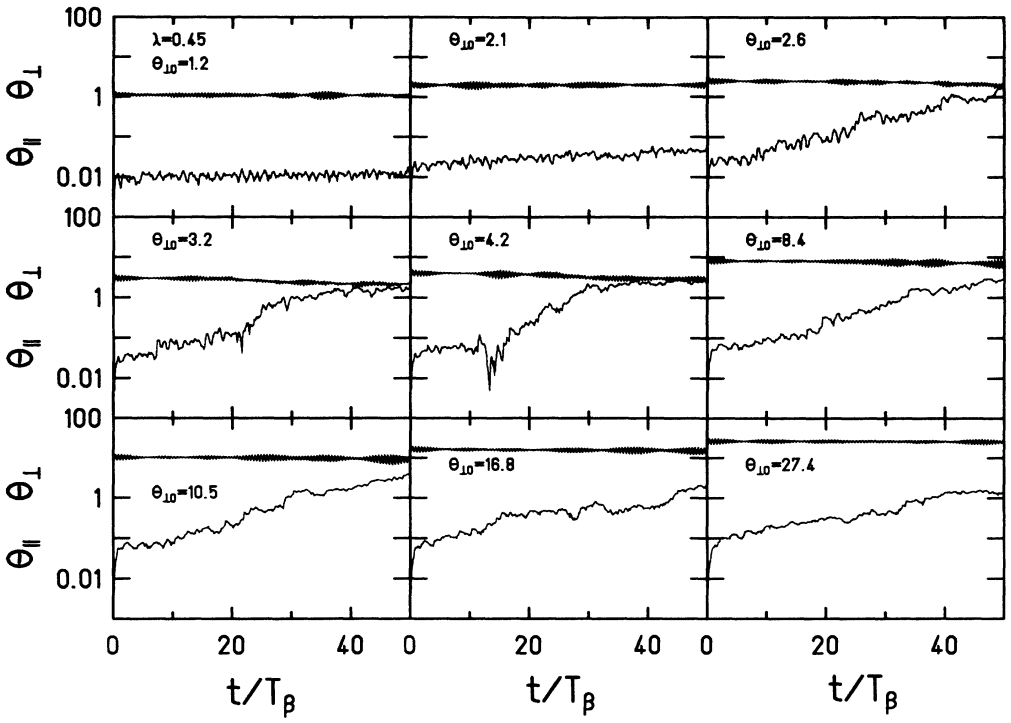

FIG. 3. Increase of longitudinal ($\Theta_\parallel$) and decrease of transverse ($\Theta_\parallel$) temperatures in time for various initial transverse temperatures ($\Theta_{\perp 0}$) and $\Theta_{\parallel 0}=0$ for a system with linear density $\lambda=0.45$. Note the logarithmic scale.

is constant since the time scale for longitudinal motion is T_0 rather than T_β. This value is well attained in the MD simulations, see Fig. 4.

In Appendix B is derived the approximate formula

$$\Theta_\parallel(t)=\Theta_{\parallel 0}+(t/t^{\text{trans}})^2\left(\tfrac{3}{2}\lambda^6\Theta_{\perp 0}^2-\tfrac{1}{2}\Theta_{\parallel 0}\right) \tag{8}$$

for the longitudinal transient heating, which is valid for not too large densities. Transient heating thus vanishes or becomes negative if $3\lambda^6\Theta_{\perp 0}^2-\Theta_{\parallel 0}<0$. This is confirmed in the MD results of Fig. 5, where the limiting value is $\Theta_{\parallel 0}=2\times 10^{-4}$ for this particular case. The plateau value of the transient energy thus becomes

$$\Theta_\parallel^{\text{trans}}=\tfrac{3}{2}\lambda^6\Theta_{\perp 0}^2. \tag{9}$$

The plateau energies for transient heating are shown in Fig. 6 and are compared with Eq. (9). The strong density dependence with the sixth power of λ is well reproduced over many decades, but for larger $\Theta_{\perp 0}$ nonlinear effects come in at the higher densities.

The maximum transient longitudinal heating calculated is about 0.01, which, for the example of Sec. I, corresponds to a beam temperature of 2.5 meV, i.e., it is of the same order of magnitude as the minimum temperature expected after electron cooling.

V. HEATING RATES

After the system has settled in its 3D state in the short transient time, a slow, approximately linear, heating of the longitudinal motion takes over. An example is shown

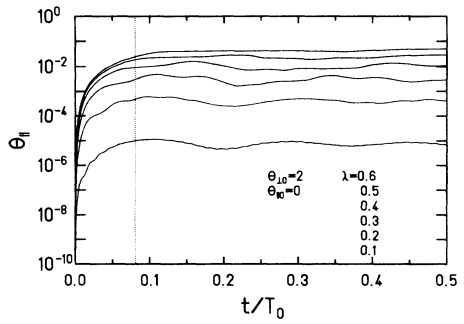

FIG. 4. Longitudinal transient heating for various densities and $\Theta_{\perp 0}=2$ and $\Theta_{\parallel 0}=0$. The dotted line marks the theoretical value.

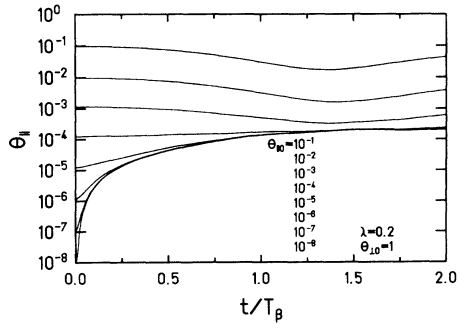

FIG. 5. Longitudinal transient heating for various initial longitudinal temperatures and $\lambda=0.2$ and $\Theta_{\perp 0}=1$. For clarity, the curves are polynomial smoothed.

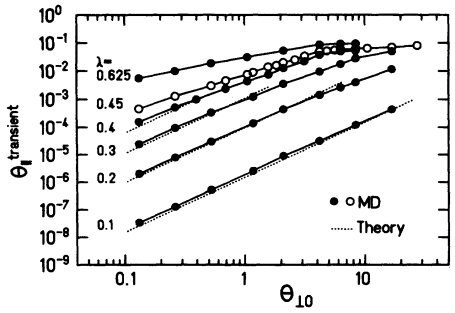

FIG. 6. Longitudinal transient plateau energies for various initial longitudinal temperatures and densities and $\Theta_{\parallel 0} = 0$. The dotted lines are theoretical results from Eq. (9).

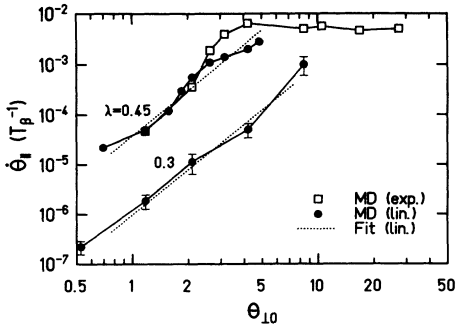

FIG. 8. Longitudinal heating rates in the linear and exponential heating regimes in units of T_β^{-1}. The dotted line is the best fit of the linear heating rate.

in Fig. 7. Here, for about 200 betatron periods, the heating rate is almost linear apart from the fact that after about 100 T_β a close encounter of two particles increased slightly the energy irreversibly. This effect has also been observed in Ref. [18]. In the MD calculations the linear heating regime was only found for densities $\lambda \geq 0.3$. For smaller densities no increase in longitudinal energy could be measured within a few hundred T_β.

The systematics with the initial transverse energy of the linear heating rate is shown in Fig. 8 for two densities. Here the dotted lines give the best fit to the data,

$$\dot{\Theta}_{\parallel} T_\beta = 0.05 \lambda^9 \Theta_{\perp 0}^3. \tag{10}$$

A theory for the linear heating rate will be the subject of a separate work.

VI. THERMALIZATION

As can be seen from the example of Fig. 7, the linear heating regime ends abruptly (at a time t^{thres} and at the threshold temperature $\Theta_{\parallel}^{thres}$) and the heating rate becomes exponential, leading to a rapid and complete thermal equilibrium when the longitudinal and the transverse temperatures become equal. The exponential heating rates have been extracted from the $\lambda = 0.45$ MD data by fits to $\Theta_{\parallel} = \Theta_{\parallel}^{trans} \exp[\gamma_{\parallel} t]$ and $\dot{\Theta}_{\parallel} \approx \gamma_{\parallel} \Theta_{\parallel}^{trans}$. They are also shown in Fig. 8 and are of the same order of magnitude as the linear ones.

The threshold times and energies are shown in Fig. 9 for $\lambda = 0.45$. After about 1.5% of the initial transverse temperature is transferred into the beam direction the exponential heating takes over. With increasing $\Theta_{\perp 0}$ this threshold time decreases rapidly down to about ten betatron periods. Accordingly, the total time for reaching thermal equilibrium of Fig. 10 drops to a few tens of betatron periods but increases again for larger initial $\Theta_{\perp 0}$. For $\Theta_{\perp 0} \geq 7$ no thermal equilibrium has been reached even after a few hundred T_β. This effect is explained in Appendix C by the fact that when the average rms transverse amplitude of Eq. (6) approaches the value $d/2$ the potential energy of the system favors large longitudinal displacements. This happens for all temperatures larger than

$$\Theta_{\perp 0}^{TE} \approx \tfrac{9}{32} \lambda^{-3}. \tag{11}$$

For $\lambda = 0.45$ this yields the value $\Theta_{\perp 0}^{TE} \approx 3$, i.e., about at the minimum of Fig. 10.

The increase in the time for thermal equilibrium beyond $\Theta_{\perp 0} \approx 4$ of Fig. 10 may be due to the fact that the longitudinal motion becomes overdamped according to Eq. (C3). In addition, relaxation times in the gaseous

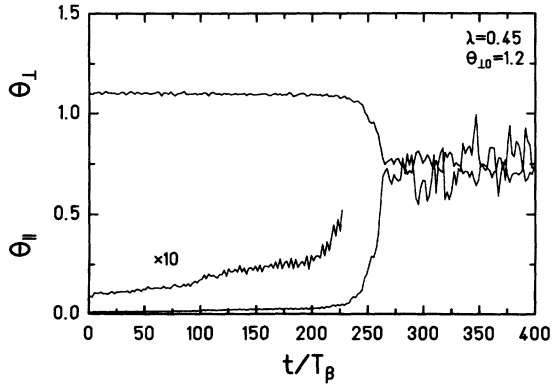

FIG. 7. Transverse ($\Theta_\perp$) and longitudinal ($\Theta_\parallel$) temperatures vs time (in units of the betatron period) for $\lambda = 0.45$ and $\Theta_{\perp 0} = 1.2$. For clarity, the results are smoothed over $\pm 2\ T_\beta$.

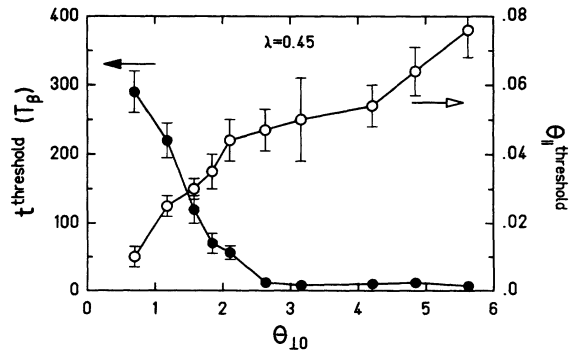

FIG. 9. Threshold times in units of the betatron period (left scale) and transverse threshold temperatures (right scale) where the exponential heating regime starts ($\lambda = 0.45$).

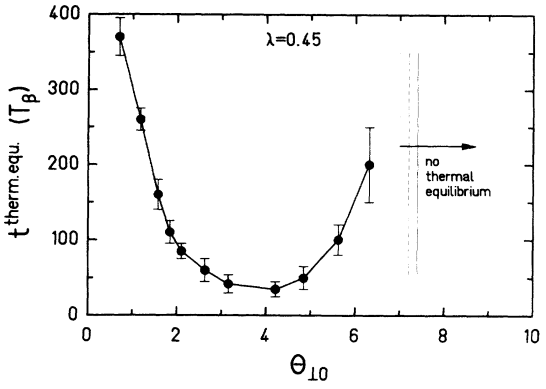

FIG. 10. Times in units of the betatron period for reaching complete thermal equilibrium in the longitudinal and transverse degrees of freedom ($\lambda=0.45$).

(high-temperature) regime increase quadratically with the temperature, cf. Ref. [22].

VII. COLLECTIVE MOTION

As discussed above, during the evolution of the system towards thermal equilibrium the uncorrelated longitudinal amplitudes can become arbitrarily large. This means that particles can change their places in the string (in our MD calculations this was observed for $\Theta_{\perp 0} > 1.2$ at a density of $\lambda = 0.45$) not only singly but also collectively. On the other hand, the saddle point for the shortest-wavelength 2^+ collective mode, where particles can change their places without loss of energy lies even lower at an energy of $0.8\epsilon_0$, even for $\rho \approx \pm 0.25$; see Appendix A. As a result, strong collective correlations are energetically favored and, accordingly, the system moves towards smaller wave numbers (larger wavelengths) in the dispersion diagram of Fig. 13 of Appendix A.

A quantitative measure for this effect are the Fourier coefficients (or phonon amplitudes) $a_\parallel(q)$ and $\dot{a}_\parallel(q)$, respectively. For complete thermal equilibrium of a harmonic system of particles they obey the relations

$$\langle |a^2(q)| \rangle = kT/2m\Omega^2(q), \qquad \langle |\dot{a}^2| \rangle = kT/2m, \quad (12)$$

where T is the temperature; see Avilov and Hofmann [20]. The long-wavelength limit of the longitudinal string frequency is given by Eq. (A6). For a finite number of particles N, however, the wave number is limited to $q_{\min} = 2\pi/Nd$. The Fourier coefficients of the transverse displacements and velocities are shown in Fig. 11 and it can be seen that already after 5 T_β the $|a_\parallel(q)|$ distribution tends towards $q \to 0$, whereas the distribution $|\dot{a}_\parallel(q)|$ remains flat, in accordance with Eq. (12). The Fourier coefficients of the transverse displacements and velocities not shown here, on the other hand, remain random for all times due to the fact that the dispersion relation is rather independent of frequency for the densities under consideration, i.e., not too close to the critical density.

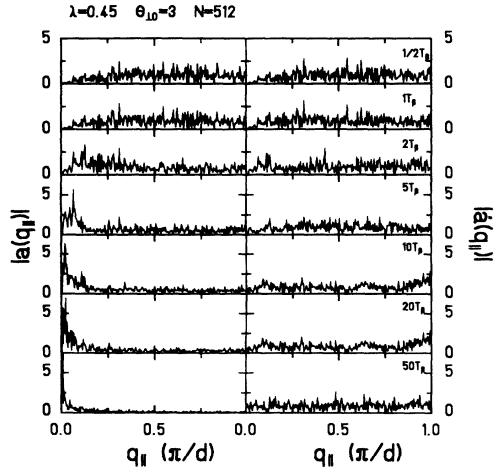

FIG. 11. Longitudinal displacement and velocity Fourier components or phonon amplitudes (in arbitrary units) vs the wave number in units of π/d ($\lambda=0.45$ and $\Theta_{\perp 0} = 3$).

VIII. SUMMARY AND DISCUSSION

The MD simulations of the exchange of energy of a transversely warm string into the initially cold beam direction revealed that this happens on different time scales, depending on the density and the initial transverse temperature. After a fraction of a betatron period the initially separated 1D longitudinal and the 2D transverse systems join in a 3D common one with transient energies that go with the sixth power of the linear density. Then the beam direction heats up with a heating rate that goes with the ninth power of the linear density until thermal equilibrium is reached. Thereby linear order is reasonably maintained, unless the initial transverse temperature is too large so that the average transverse amplitude is of the order of the interparticle spacing. In this case heating times become as small as a few betatron periods.

In the other extreme of low density and low temperature, heating times can reach a few thousand T_β. From the transient energy (9) and the fit to the linear heating rate (10) (which is about equal to the one with the exponential heating rate) one derives an approximate formula for the e-folding time $\tau_{\text{heat}} = \Theta_\parallel^{\text{trans}}/\dot{\Theta}_\parallel$ for longitudinal heating,

$$\tau_{\text{heat}} \approx \frac{30}{\lambda^3 \Theta_{\perp 0}} T_\beta. \quad (13)$$

For $\Theta_{\perp 0} = 5$ and $\lambda = (0.3, 0.2, 0.1)$ this is of the order of $(200, 750, 6000)$ T_β. This heating rate has to be neutralized by the electron cooler in the storage ring. We therefore have simulated the effect of the electron cooler in the MD calculations by adding a cooling force in the beam direction which has the effect of reducing the longitudinal temperature by certain cooling rates. Indeed, $\Theta_\parallel$ remains stationary at the level of $\Theta_\parallel^{\text{trans}}$ if the cooling rate is about equal to the heating rate.

The electron cooler in the ESR at GSI Darmstadt is expected to achieve typical cooling times of 20 000 T_β (cooling times are of the order of a few milliseconds). Hence λ must be as small as possible, which, according

to Eq. (4), can only be achieved by strong focusing. This in turn means that the betatron tune Q, the ratio of betatron frequency to revolution frequency $\omega_{\rm rev}$, must be as large as possible. As an example, for a $^{238}U^{92+}$ beam at 500 MeV per particle the Lorentz factor is $\gamma = 1.5$. With an interparticle distance of 50 μm one has $\omega_0 = 3$ MHz and $\omega_{\rm rev} = 13$ MHz. In order to achieve $\lambda = 0.1$ (0.2), Q must be of the order of 10 (3). By virtue of the geometric structure of a storage ring imposed by the number of focusing and defocusing magnets and by the increasing number of resonances the betatron tune is limited to values around $Q < 4$. In conclusion, it is marginal to achieve such low linear densities of $\lambda \approx 0.1$ where the electron cooling rate can neutralize the expected longitudinal heating rate.

There are, however, other mechanisms that also contribute to heating the beam longitudinally, e.g., the influence of nonideal beam optics, of scattering with the rest gas, and of electron recombination in the cooler. Ideal radial harmonic focusing, as assumed above, cannot be realized by focusing and defocusing quadrupole magnets; and, even more serious, the bending dipole magnets act to destroy longitudinal order by virtue of the shearing stress created at higher transverse temperatures. As a first step towards more realistic simulations we replaced the constant radial focusing force by cyclic $F0D0$. However, apart from the fact that these external time-dependent forces no longer conserve the total energy and hence the final $\Theta_\parallel$ no longer equals $\frac{2}{3}\Theta_{\perp 0}$, no drastic differences were found in the heating rates. Such studies with a realistic lattice of a storage ring including the bending magnets are underway.

Scattering with the rest gas, on the other hand, results mainly in a deceleration of the beam, see [16]. Without relativistic factors this is approximately

$$\dot{E} \approx 10 E_0 Z^2 [p_{\rm H_2}({\rm Torr})]\ {\rm sec}^{-1}, \tag{14}$$

where $p_{\rm H_2} \approx 10^{-10}$Torr is the hydrogen equivalent rest-gas pressure. This theoretical formula has been derived from Rutherford scattering and yields a value of the order of 2 meV/T_β. It compares with the experimental value of ≈ 50 μeV/T_β derived from the fact that the lifetime of a heavy-ion beam in the ESR is of the order of 1 h before it loses about 1% of its energy per particle E_0. This energy loss is compensated for by the electron cooler. The thermal heating of the beam due to scattering with the rest gas, on the other hand, is a second moment effect and as such is expected to be at least an order of magnitude smaller with heating times of at least $10^6\ T_\beta$.

ACKNOWLEDGMENT

The author acknowledges fruitful discussions with V.V. Avilov and I. Hofmann.

APPENDIX A: STRING VIBRATIONS

Denoting the longitudinal amplitude of particle n by $u_n(t)$, viz., $z_n(t) = nd + u_n(t)$, under the approximations $|u_i - u_j|, |\rho_i - \rho_j| \ll d$ the accelerations in longitudinal and transverse directions in the laboratory system can be expanded as

$$\begin{aligned}\gamma^2 \ddot{u}_n = \omega_0^2 \sum_{k>0} \Bigg(& -\frac{1}{k^3}[2u_n - u_{n-k} - u_{n+k}] - \frac{3}{2dk^4}[(u_n - u_{n-k})^2 - (u_n - u_{n+k})^2] \\ & + \frac{3}{4dk^4}[(\rho_n - \rho_{n-k})^2 - (\rho_n - \rho_{n+k})^2] - \frac{2}{d^2k^5}[(u_n - u_{n-k})^3 + (u_n - u_{n+k})^3] \\ & + \frac{3}{d^2k^5}\Big[u_n((\rho_n - \rho_{n-k})^2 + (\rho_n - \rho_{n+k})^2) - u_{n-k}(\rho_n - \rho_{n-k})^2 - u_{n+k}(\rho_n - \rho_{n+k})^2\Big] + \dots \Bigg),\end{aligned} \tag{A1}$$

$$\begin{aligned}\ddot{\rho}_n = -\omega_\beta^2 \rho_n + \omega_0^2 \sum_{k>0} \Bigg(& \frac{1}{2k^3}[2\rho_n - \rho_{n-k} - \rho_{n+k}] - \frac{3}{2dk^4}[(\rho_n - \rho_{n-k})(u_n - u_{n-k}) - (\rho_n - \rho_{n+k})(u_n - u_{n+k})] \\ & + \frac{3}{d^2k^5}[(\rho_n - \rho_{n-k})(u_n - u_{n-k})^2 + (\rho_n - \rho_{n+k})(u_n - u_{n+k})^2] \\ & - \frac{3}{4d^2k^5}[(\rho_n - \rho_{n-k})^3 + (\rho_n - \rho_{n+k})^3] + \dots \Bigg).\end{aligned} \tag{A2}$$

The respective first terms are the harmonic contributions which, for uncorrelated (i.e., random) motion give the frequencies

$$\gamma\Omega_\parallel = \sqrt{2\zeta_3}\,\omega_0, \qquad \Omega_\perp = \sqrt{\omega_\beta^2 - \zeta_3 \omega_0^2}. \tag{A3}$$

Here $\zeta_n = \sum_{k=1}^{\infty} k^{-n}$ is the Riemann zeta function. For collective motion, on the other hand, the modes of vibration can be classified by a mode number M or wave number $q = 2\pi/Md$ and the parity Π according to cosinelike or sinelike vibrations in longitudinal or transverse directions,

$$\left.\begin{aligned} z_n &= nd + u\left\{\begin{matrix}\cos\\ \sin\end{matrix}\right\}(nqd) \\ \rho_n &= \rho\left\{\begin{matrix}\cos\\ \sin\end{matrix}\right\}(nqd)\end{aligned}\right\} \quad \text{for} \quad \Pi = \left\{\begin{matrix}+\\ -\end{matrix}\right\}. \tag{A4}$$

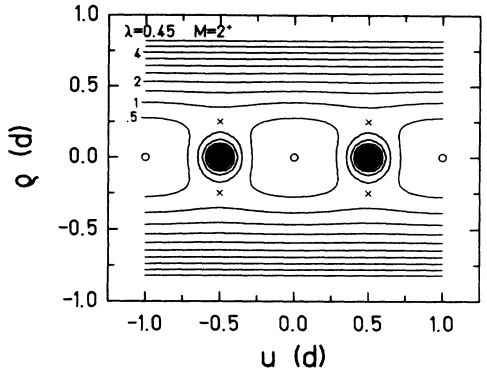

FIG. 12. Contour plot of the potential energy per particle for collective $M=2^+$ oscillations of the longitudinal and transverse displacements u and ρ. Circles are ground states at zero energy and crosses are saddle points. Contour lines are spaced by $0.5q^2/d$.

Here $M=2^+$ is the lowest interesting mode, the zigzag mode. According to the symmetry of q in Eq. (A4), the intervals $0\le qd\le\pi$ or $2\le M\le\infty$ suffice. The potential energy for $M=2^+$ vibrations is shown in Fig. 12. The saddle point here is reached for $\rho\approx\pm0.25d$ and has an energy of $0.8\epsilon_0$.

In the small-amplitude (harmonic) limit the eigenfrequencies are degenerate in parity. The longitudinal frequencies read

$$\gamma\Omega_\parallel(q)=\omega_0\sqrt{8\sum_{n=1}^{\infty}n^{-3}\sin^2\tfrac{1}{2}nqd}$$

and the maximum longitudinal frequency is attained for the zigzag 2^+mode, i.e., at $qd=\pi$,

$$\gamma\Omega_\parallel(\pi)/\omega_0=\sqrt{7\zeta_3}=2.9; \tag{A5}$$

and in the long-wavelength limit,

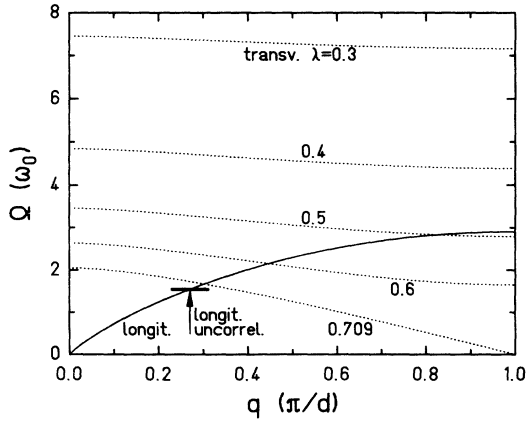

FIG. 13. Dispersion relation Eq. (A6) for correlated longitudinal (full line) and transverse (dotted line for various densities λ) motion and for uncorrelated longitudinal motion (bar).

$$\gamma\Omega_\parallel(q\to0)/\omega_0=qd\sqrt{2\ln(1/qd)}. \tag{A6}$$

The transverse frequencies, on the other hand, depend on the density λ, and $\Omega_\perp(\pi)$ vanishes at $\lambda_{\rm crit}$ where the string ceases to be the energetically lowest configuration (the transition to the stable zigzag structure). They follow from the dispersion relation

$$\gamma^2\Omega_\parallel^2(q)+2\Omega_\perp^2(q)=2\omega_\beta^2, \tag{A7}$$

so that $\Omega_\perp(0)=\omega_\beta$. The maximum density a Coulomb string can tolerate before it turns into a stable zigzag is reached if $\Omega_\perp=0$. With the help of Eq. (4) this yields the value $\lambda_{\rm crit}=[3/7\zeta_3]^{1/3}=0.709$. Equation (A7) is also valid for uncorrelated motion. These dispersion relations are shown in Fig. 13.

APPENDIX B: TRANSIENT HEATING MODEL

For uncorrelated (statistical) longitudinal and transverse initial conditions (in contrast to collective motion) every particle oscillates harmonically with the longitudinal frequency $\Omega_\parallel$ and the transverse one $\Omega_\perp$ (approximately the betatron frequency), cf. Eqs. (A3). Initially, the force in the third line of Eq. (A1) is harmonic with twice the transverse frequency $\Omega_\perp$ and can be written as $A_n+B_n\cos2\Omega_\perp t+C_n\sin2\Omega_\perp t$. Its statistical average vanishes, $\langle A_n\rangle=\langle B_n\rangle=\langle C_n\rangle=0$, as well as its time average. For short times, however, it kicks each particle at random in the longitudinal direction and, since

$$\begin{aligned}&\langle A_n^2\rangle=\langle B_n^2\rangle=\langle C_n^2\rangle=3\zeta_4^2\lambda^6\omega_0^4d^2\Theta_{\perp0}^2,\\&\langle(A_n-\tfrac{1}{2}A_{n-1}-\tfrac{1}{2}A_{n+1})^2\rangle=\tfrac{25}{4}\zeta_4^2\lambda^6\omega_0^4d^2\Theta_{\perp0}^2,\end{aligned} \tag{B1}$$

it gives the transient contribution to the longitudinal heating. The equation of motion for u_n becomes the one of a driven harmonic oscillator,

$$\ddot u_n+\Omega_\parallel^2u_n=A_n+B_n\cos2\Omega_\perp t+C_n\sin2\Omega_\perp t+\frac{1}{2}\Omega_\parallel^2(u_{n-1}+u_{n+1}),$$

and can be integrated (the Lorentz factor here is omitted). The leading contributions in lowest order in powers of $(\omega_0/\omega_\beta)^2$ [equal to $\frac{2}{3}\lambda^3$ according to Eq. (4)] and with only the nearest-neighbor interactions ($k=1$), reads

$$\dot u_n=\dot u_{n0}\cos\Omega_\parallel t+(A_n-\tfrac{1}{2}A_{n-1}-\tfrac{1}{2}A_{n+1})\frac{\sin\Omega_\parallel t}{\Omega_\parallel}+\frac{2\omega_\beta}{4\omega_\beta^2-\Omega_\parallel^2}\Big(C_n\cos\Omega_\parallel t+B_n\sin2\omega_\beta t-C_n\cos2\omega_\beta t\Big),$$

where $\dot u_{n0}$ are the random initial velocities (the initial displacements are vanishing). Remembering that $\langle\dot u_n^2\rangle=\omega_0^2d^2\Theta_\parallel$, the kinetic energy becomes

$$\Theta_\parallel(t)=\Theta_{\parallel0}\cos^2\Omega_\parallel t+\tfrac{25}{8}\frac{\zeta_4^2}{\zeta_3}\lambda^6\Theta_{\perp0}^2\sin^2\Omega_\parallel t.$$

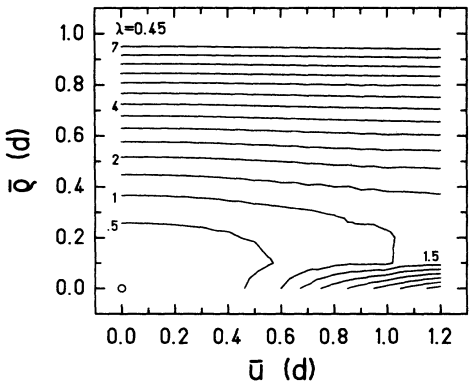

FIG. 14. Contour plot of the potential energy per particle vs the mean longitudinal and transverse displacements $\bar{u}$ and $\bar{\rho}$. Contour lines are spaced by $0.5q^2/d$.

For short times, $\Omega_\parallel t \ll 1$, this becomes

$$\Theta_\parallel(t) = \Theta_{\parallel 0} + (\Omega_\parallel t)^2 \left(\tfrac{25}{8} \frac{\zeta_4^2}{\zeta_3} \lambda^6 \Theta_{\perp 0}^2 - \Theta_{\parallel 0} \right). \quad \text{(B2)}$$

Averaging over long-time intervals $2\pi/\Omega_\parallel$, on the other hand, gives the average value

$$\Theta_\parallel^{\text{trans}} = \tfrac{1}{2}\Theta_{\parallel 0} + \tfrac{25}{16}\lambda^6 \Theta_{\perp 0}^2. \quad \text{(B3)}$$

Transient times are of the order of the ratio of average interparticle distance to average longitudinal interparticle velocity, cf. [22], viz., $\Omega_\parallel t^{\text{trans}} \approx 1$. In the MD simulations, see Fig. 4, the asymptotic value (B3) is already reached for $\Omega_\parallel t^{\text{trans}} \approx 2^{-1/2}$, i.e., after one-eighth Coulomb period. With $25\zeta_4^2/16\zeta_3 = 1.52$ this yields Eq. (8).

APPENDIX C: THERMAL EQUILIBRIUM

The Coulomb energy per particle relative to the one of the string at rest reads

$$\epsilon_{\text{Coul}} = \frac{q^2}{N} \sum_i \sum_{j>i} \left(|\mathbf{r}_j - \mathbf{r}_i|^{-1} - [jd - id]^{-1} \right). \quad \text{(C1)}$$

Averaged over the equally probable angle between $\boldsymbol{\rho}_i$ and $\boldsymbol{\rho}_j$, the argument of Eq. (C1) simplifies to

$$\overline{|\mathbf{r}_j - \mathbf{r}_i|^{-1}} = \frac{k_{ij} K(k_{ij})}{\pi \sqrt{\rho_i \rho_j}}, \quad \text{(C2)}$$

where $K(k^2)$ is the complete elliptic integral of the modulus

$$k_{ij}^2 = \frac{4\rho_i \rho_j}{\sqrt{([j-i]d - u_i + u_j)^2 + (\rho_i - \rho_j)^2 + 4\rho_i \rho_j}}.$$

The potential energy of an uncorrelated system, i.e., the Coulomb energy [(C1) and (C2)] plus the focusing energy,

$$\epsilon_{\text{focus}} = \frac{m\omega_\beta^2}{2N} \sum_i \rho_i^2,$$

are computed for 1024 particles with Gaussian distributed longitudinal and transverse displacements with their respective mean values $\bar{u} = \langle u^2 \rangle^{1/2}$, and $\bar{\rho}$ and is shown in Fig. 14. Approximately for $2\bar{\rho} > \bar{u}$ the Coulomb energy vanishes or becomes negative, and thus for all $\bar{\rho} > d/2$ the potential energy consists mainly of the focusing energy, which is independent of $\bar{u}$, thus indicating that the system can sustain large longitudinal displacements. This, in turn, means that the system has vaporized and thermal equilibrium has been reached. According to Eq. (6) and taking account of the fact that at thermal equilibrium $\Theta_\perp^{\text{te}} = \frac{2}{3}\Theta_{\perp 0}$, we derive Eq. (11).

In the small-amplitude limit the unharmonic terms in Eq. (A1) give rise to a modification of the longitudinal (and transverse, as well) frequency which can be written as

$$\langle \Omega_\parallel{}^2 \rangle = \omega_0^2 \left(2\zeta_3 + 16\zeta_5 \frac{\langle u^2 \rangle}{d^2} - 12\zeta_5 \frac{\langle \rho^2 \rangle}{d^2} \right).$$

This can become negative if

$$\langle \rho^2 \rangle > \frac{\zeta_3}{6\zeta_5} + \tfrac{4}{3}\langle u^2 \rangle, \quad \text{(C3)}$$

and hence the longitudinal motion can become overdamped. Furthermore, in the high-temperature limit relaxation times increase with the square of the temperature, cf. [22].

[1] J.P. Schiffer and P. Kienle, Z. Phys. A **321**, 181 (1985).
[2] J.P. Schiffer and O. Poulsen, Europhys. Lett. **1**, 55 (1986).
[3] S. Ichimaru, Rev. Mod. Phys. **54**, 1017 (1982).
[4] H.E. DeWitt, W.L. Slattery, and S. Stringfellow, in *Proceedings of the 24th Yamada Conference on Strongly Coupled Plasmas, Lake Yamanaka, 1989*, edited by S. Ichimaru (North-Holland-Elsevier, New York, 1990), p. 635.
[5] A. Rahman and J.P. Schiffer, Phys. Rev. Lett. **57**, 1133 (1986).
[6] A. Rahman and J.P. Schiffer, in Proceedings of the Workshop and Symposium on the Physics of Low-energy Stored and Trapped Particles, Stockholm 1987, edited by A. Bárány, A. Kerek, M. Larsson, S. Mannervik, and L.-O. Norlin [Phys. Scrip. **T22**, 133 (1988)].
[7] R.W. Hasse and J.P. Schiffer, Ann. Phys. **203**, 419 (1990).
[8] R.W. Hasse, Phys. Rev. Lett. **67**, 600 (1991).
[9] M.G. Raizen, J.M. Gilligan, J.C. Bergquist, W.M. Itano, and D.J. Wineland, J. Mod. Opt. **39**, 233 (1992).
[10] I. Waki, S. Kassner, G. Birkl, and H. Walther, Phys. Rev. Lett. **68**, 2007 (1992).

[11] J.P. Schiffer and A. Rahman, Z. Phys. A **331**, 71 (1988).
[12] J.P. Schiffer, in GSI Darmstadt Report No. 89-10, 1989 (unpublished), p.2.
[13] R.W. Hasse, in *Proceedings of the First Kiev International School on Nuclear Physics, Kiev, 1990*, edited by O.F. Nemets and A.T. Rudchik (Kiev Naukoma Dumka, Kiev, 1991), p. 316.
[14] D. Habs *et al.*, Nucl. Instrum. Methods B **43**, 390 (1989).
[15] S. Schröder *et al.*, Phys. Rev. Lett. **64**, 2901 (1990).
[16] H. Poth, Phys. Rep. **196**, 135 (1990).
[17] P. Spädtke *et al.*, GSI Nachrichten No. 12-90, 1990 (unpublished), p.17.
[18] J.P. Schiffer and J.S. Hangst, Z. Phys. A **341**, 107 (1991).
[19] G. Armbrüster, B. Majer, U. Reimann, and C. Toepffer (unpublished).
[20] V.V. Avilov and I. Hofmann (unpublished).
[21] In contrast to our results, in Ref. [18] transient times are about 5 T_β.
[22] S. Ichimaru, *Basic Priciples of Plasma Physics* (Benjamin, New York, 1973), Chap. 10.